Synthesis and Evaluation of Novel Macrocyclic and Acyclic Ligands as Contrast Enhancement Agents for Magnetic Resonance Imaging

Hyun-Soon Chong,*[†,‡] Kayhan Garmestani,[‡] L. Henry Bryant, Jr.,[§] Diane E. Milenic,[‡] Terrish Overstreet,[‡] Noah Birch,[†] Thien Le,[†] Erik D. Brady,[‡] and Martin W. Brechbiel[‡]

Biological, Chemical, and Physical Sciences Department, Chemistry Division, Illinois Institute of Technology, Chicago, Illinois 60616, Radioimmune and Inorganic Chemistry Section, Radiation Oncology Branch, Center for Cancer Research, National Cancer Institute, Bethesda, Maryland 20892, and Diagnostic Radiology Department, Clinical Center, National Institutes of Health, Bethesda, Maryland 20892

Novel chelates PIP−DTPA, AZEP−DTPA, NETA, NPTA, and PIP−DOTA were synthesized and evaluated as potential magnetic resonance imaging (MRI) contrast enhancement agents. The T_1 and T_2 relaxivities of their corresponding Gd(III) complexes are reported. At clinically relevant field strengths, the relaxivities of the complexes are comparable to that of the clinically used contrast agents Gd(DTPA) and Gd(DOTA). The serum stability of the ^{153}Gd-labeled complexes, Gd(PIP−DTPA), Gd(AZEP−DTPA), Gd(PIP−DOTA), Gd-(NETA), and Gd(NPTA), was assessed by measuring the release of ^{153}Gd from the complexes. ^{153}Gd-(NETA), ^{153}Gd(PIP−DTPA), and ^{153}Gd(PIP−DOTA) were found to be stable in human serum for up to 14 days without any measurable loss of radioactivity. Significant release of ^{153}Gd was observed with the ^{153}Gd-(III) radiolabled NPTA. In vivo biodistribution of the^{153}Gd-labeled complexes was performed to evaluate their in vivo stability. While Gd(AZEP−DTPA) and Gd(NPTA) were found to be unstable in vivo, Gd(NETA), Gd(PIP−DTPA), and Gd(PIP−DOTA) were excreted without dissociation. These results suggest that the Gd(III) complexes of the novel chelates NETA, PIP−DTPA, and PIP−DOTA possess potential as MRI contrast enhancement agents. In particular, the piperidine backboned chelates Gd(PIP−DTPA) and Gd(PIP−DOTA) displayed reduced kidney retention as compared to the nonspecific MRI contrast agent Gd(DOTA) at all time points, although the observed effects were relatively small at 0.5 h postinjection. Incorporation of the lipophilic piperidine ring appears to confer a moderate effect on the liver uptake of these two chelates.

Introduction

Magnetic resonance imaging (MRI), a noninvasive and high-resolution imaging technique, has become a powerful tool in diagnostic medicine.[1] MRI gives distribution of the MR signal intensity resulting from the longitudinal (T_1) and the transverse (T_2) magnetic relaxation time of tissue water protons.[2] The images with a clear contrast between tissues with different relaxation times of water protons T_1 and T_2 can be obtained with MRI. However, the innate tissue contrast in images is not sufficient to distinguish between normal and pathogenic tissues when they produce similar signal intensity. To enhance contrast between tissues, paramagnetic metal complexes are injected into the body and lead to significant improvement in the contrast of T_1-weighted or T_2-weighted MR image by increasing the difference in the signal intensity from two different types of tissues.[3]

The lanthanide Gd(III) is known to be an optimal paramagnetic metal for MRI because of high electronic spin ($^7/_2$) and slow electronic relaxation rate.[4] Free Gd(III), however, is toxic with severe side effects.[5] Thus, stable Gd(III) complexes are required for in vivo use with efficient excretion postadministration. A number of Gd(III) complexes such as Gd(DOTA) and Gd(DTPA) (Figure 1) are clinically approved for use in MRI.[2] However, most contrast agents have nonspecific extra-cellular distribution and the disadvantages of low relaxivity, low tissue specificity, and rapid clearance. Considerable research efforts have been directed toward developing safe Gd(III)-based MR contrast agents with high tissue specificity and sensitivity.

MRI is proven to be more sensitive and specific than other medical tests for detecting liver malignancies and for distinguishing them from benign lesions.[7] The gadolinium complexes of BOP−DTPA and EOB−DTPA (Figure 1) are the clinically approved hepatobiliary agents.[6] These agents are partially taken up by normal hepatocytes, probably due to the binding of the lipophilic aromatic moiety to cytosolic protein in the hepatocytes,[2] and this selective uptake of the agents into the normal liver cells yields enhanced contrast between normal and tumorous liver cells on T_1-weighted images.[7] The utility of these agents is in the detection and the characterization of hepatocelluar lesions.[8] However, the Gd(III) complexes provide low detection and characterization of metastatic lesions.[7]

We have recently prepared stereochemically pure piperidine (PIP−DTPA) and azepane (AZEP−DTPA) backboned DTPA derivatives as potential hepatocellular agents (Figure 2).[9a] Our strategy in the design of the chelates was to increase lipophilicity and rigidity of the chelate system by incorporating either a piperidine or an azepane ring into the DTPA system. This was anticipated to result in both enhanced hepatobiliary clearance and in vivo complex stability. In general, conformational constraint of chelating agents, i.e., inclusion of a rigid structure to control the geometry of the metal binding donor groups, has a significant effect on the stability of the formed metal complexes.[10] High lipophilicity is known to result in greater hepatobiliary clearance.[11] We previously reported that the Gd(III) complexes of the new chelates PIP−DTPA and AZEP−

* To whom correspondence should be addressed. Address: Biological, Chemical, and Physical Science Department, Chemistry Division, Illinois Institute of Technology, 3101 S. Dearborn St, LS 182, Chicago, IL 60616. Phone: 312-567-3235. Fax: 312-567-3494. E-mail: Chong@iit.edu.
† Illinois Institute of Technology.
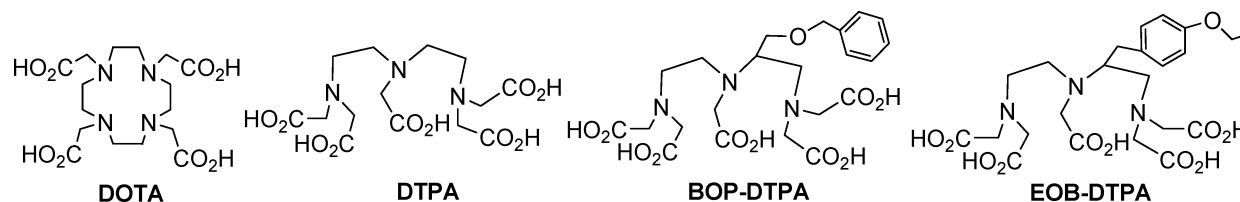‡ National Cancer Institute.
§ National Institutes of Health.

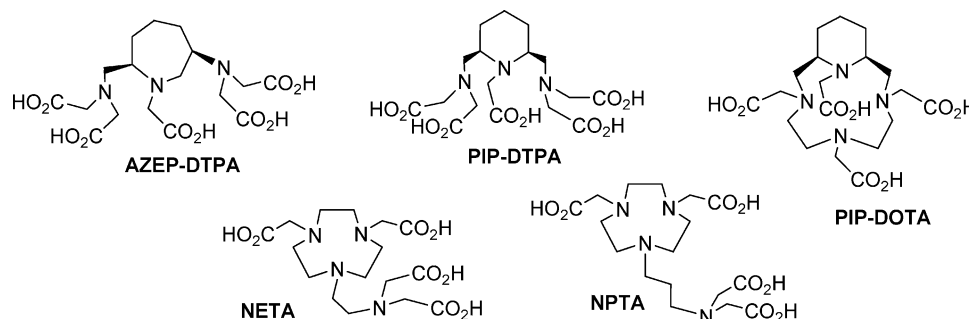**Figure 1.** Magnetic resonance imaging contrast agents in clinical use.

Figure 2. New potential Gd(III)-based magnetic resonance imaging contrast enhancement agents.

DTPA display comparable relaxivity and significantly improved in vitro stability to Gd(DTPA).[9a]

In our continuing effort to develop liver-specific contrast enhancement agents, Gd(PIP−DTPA) and Gd(AZEP−DTPA) are further evaluated for in vivo stability. Novel Gd(III) complexes of PIP−DOTA, NETA, and NPTA (Figure 2) have been prepared and evaluated. The structurally new chelates NETA and NPTA possess both macrocyclic and acyclic pendent sidearms. The dynamic participation of the pendent sidearm in NETA and NPTA in binding to Gd(III) is expected to potentially impact access and relaxivity of water protons and complex stability. A novel chelate, PIP−DOTA, possesses a liphophilic piperidine ring. The liphophilicity and rigidity of PIP−DOTA is greater than those of the parent DOTA. Like PIP−DTPA, PIP−DOTA is expected to provide enhanced hepatobiliary clearance while maintaining the complex stability of DOTA.

We herein report the synthesis and evaluation of PIP−DOTA as MRI contrast agents. We also evaluated a new series of Gd(III) chelates, PIP−DTPA, AZEP−DTPA, NETA, and NPTA. The relaxivities of the corresponding Gd(III) complexes were measured. The in vitro and in vivo stabilities of the [153]Gd-

labeled complexes of the new chelates were investigated in human serum and mice, respectively.

Results and Discussion

Synthesis of Novel Chelates. The chemical structures of the chelates PIP−DTPA, AZEP−DTPA, PIP−DOTA, NETA, and NPTA for the present study are shown in Figure 2. PIP−DTPA,[9a] AZEP−DTPA,[9a] NETA,[9b] and NPTA[9b] were prepared as described previously. The synthesis of PIP−DOTA containing a piperidine backbone is shown in Scheme 1. The key step in the synthesis of PIP−DOTA is the coupling reaction between two precursor molecules **3** and **4** to provide macrocycle **5**. This cyclization was very efficiently achieved under a high dilution condition. To accomplish this coupling route, precursor molecule **4** was prepared by reaction of ethyl glycine with excess ethylenediamine.[12] Precursor molecule **3** was prepared from the readily available 2,6-pyridinedicarboxylic acid **1**. Thus, catalytic hydrogenation of pyridine 2,6-dicarboxylic acid **1** over rhodium on alumina provided enantiomerically pure *cis*-2,6-piperidine dicarboxylic acid, which subsequently was reacted with CBZ−Cl to provide *N*-CBZ-*cis*-2,6-dicarboxylic acid **2**.[13] The diacid

Scheme 1. Synthesis of PIP−DOTA
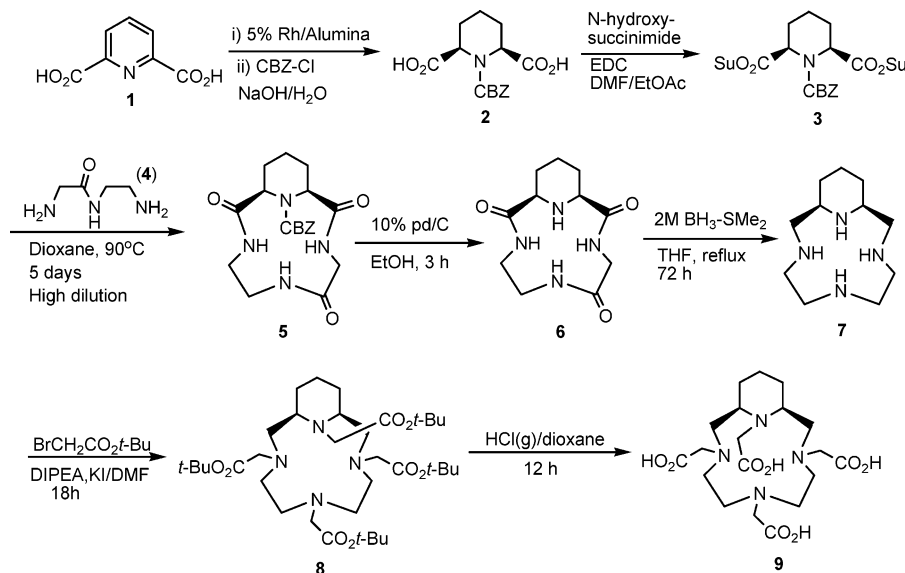
Figure 3. Plots of T_1 relaxivity for Gd(NETA) (○), Gd(NPTA) (◇), Gd(AZEP−DTPA) (●), Gd(PIP−DTPA) (◆), Gd(PIP−DOTA) (■), Gd(DTPA) (▲), and Gd(DOTA) (△) at pH 7 and 23 °C. The data for Gd(AZEP−DTPA) and Gd(PIP−DTPA) were previous results from ref 9a.
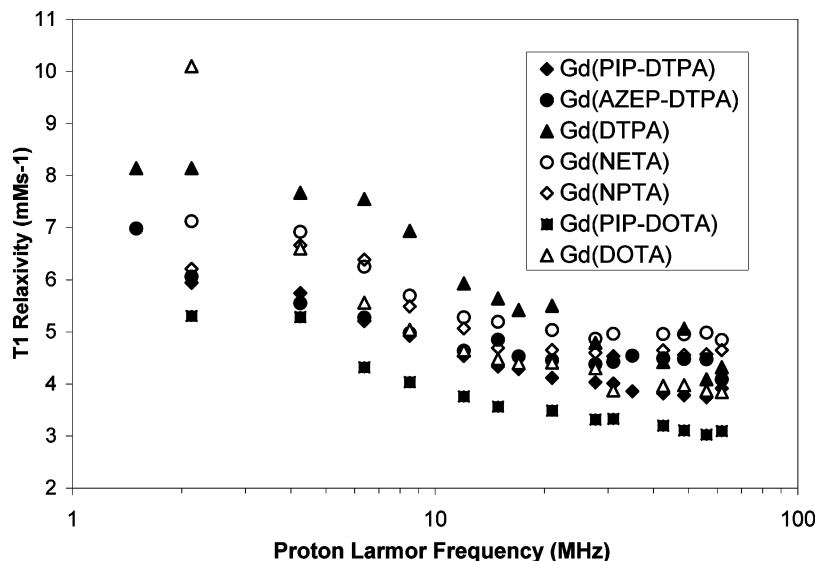

Figure 4. Plots of T_2 relaxivity for Gd(NETA) (○), Gd(NPTA) (◇), Gd(AZEP−DTPA) (●), Gd(PIP−DTPA) (◆), Gd(PIP−DOTA) (■), Gd(DTPA) (▲), and Gd(DOTA) (△) at pH 7 and 23 °C. The data for Gd(AZEP−DTPA) and Gd(PIP−DTPA) were previous results from ref 9a.
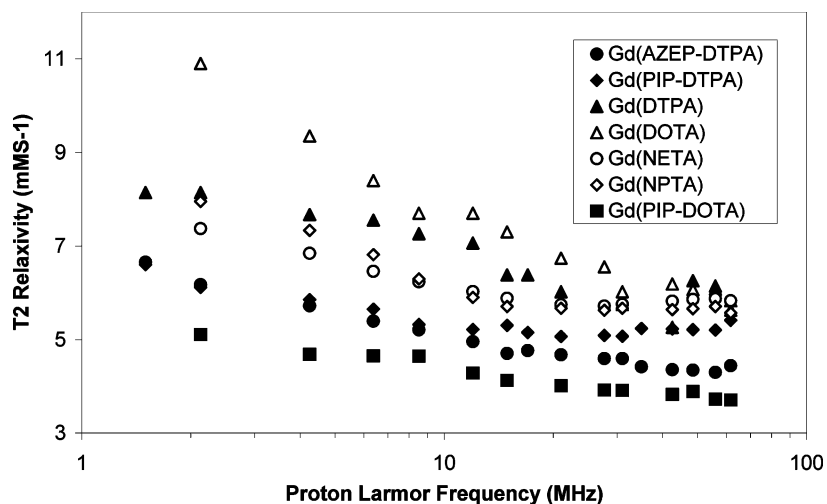
2 was converted into the activated ester **3** in 78% yield. Coupling of **3** with **4** under high dilution conditions provided piperidine-backboned macrocycle **5** in good yield (53%). The CBZ group in **5** was removed by catalytic hydrogenation over palladium to provide bicyclic triamide **6**. The reduction of carbonyl groups in **6** was attempted with 1 M BH$_3$−THF at 50 °C, initially adapting previously reported conditions.[14] However, these reaction conditions provided only a trace of **7** along with partially reduced byproducts containing a mixture of unreduced carbonyl groups adjacent to the piperidine ring as confirmed by mass and NMR spectra. A successful reduction of **6** was performed under a somewhat harsh reflux condition while changing the borane reagent. Thus, the bicyclic triamide **6** was treated with BH$_3$−SMe$_2$ complex and refluxed for 5 days to cleanly provide the cyclic tetraamine **7** (55%). For the synthesis of **8**, **7** was reacted with *tert*-butyl bromoacetate in the presence of NaCO$_3$ at 65 °C. However, these reaction conditions provided an undesired penta-alkylated quaternary byproduct as confirmed by mass ($m/z = 783.4$ [M + H$^+$]) and ^{13}C NMR (four carbonyl peaks of *tert*-butyl ester, 163.7, 169.4, 170.3, and 170.6 at a 2:1:1:1 ratio) analysis. Alkylation of the HCl salt of **7** was then carried out in DMF in the presence of DIPEA and KI at 90 °C to provide **8** as the major product in 37% yield. The *tert*-butyl

groups in **8** were removed by treating with HCl(g) to provide the desired chelate, PIP−DOTA (**9**) in 87% yield.

Relaxivity. The Gd(III) complexes of the new chelates were prepared using a described method.[9a] T_1 and T_2 NMRD profiles for the Gd(III) complexes are depicted in Figures 3 and 4, respectively. For comparison purposes, the T_1 and T_2 relaxivities of the commercially available Gd(DTPA) (Magnevist) and Gd(DOTA) (Dotarem) were measured. It appears that the T_1 NMRD profiles parallel the T_2 NMRD profiles. Qualitatively and quantitatively, the T_1 and T_2 NMRD profiles for the newly synthesized Gd(III) complexes are similar to those of the clinically used MR contrast agent GdDTPA (Magnevist) and to those of other previously reported Gd acyclic and macrocyclic complexes where the Gd(III) is coordinated to the eight donor atoms of the ligands with one vacant coordination site available to bind a water molecule.[2] In NMRD, the T_1 relaxivities of the evaluated new Gd(III) complexes at 20 MHz were comparable to that of Gd(DOTA), and the difference of relaxivity between the Gd(III) complexes are in the range of ±1.16 MHz. This supports that the number of water molecules coordinated to the Gd(III), q, is equal to 1.[2,15] The relaxation rates for the Gd(III) chelates are dominated by the inner-sphere dipolar coupling

between the coordinated water molecule and the paramagnetic Gd(III). The measured relaxivities arise from the exchange between the coordinated water molecule and the surrounding water molecules in solution. An increase in the number of coordinated water molecules to the Gd(III), which could have occurred with dissociation of the Gd(III) from the chelate in solution, would have resulted in a significant increase in the measured relaxivities. No indication of Gd(III) dissociation is evident from the NMRD profiles, which is in agreement with the serum stability studies. In a previous study, we reported that Gd(PIP−DTPA) and Gd(AZEP−DTPA) display comparable relaxivity to Gd(DTPA) at the clinically relevant field strength, 61 MHz. Examination of the NMRD profiles at around 15 MHz provides evidence that the T_1 and T_2 relaxivities are dominated by the rotational correlation time (tumbling time) of these low molecular weight compounds.[16] Inspection of T_1 and T_2 relaxivities at 60 MHz in Figures 3 and 4 indicates that among the evaluated Gd(III) complexes, Gd(NETA) gives the highest T_1 and T_2 relaxivity at 61 MHz, while PIP−DOTA gives the lowest T_1 and T_2 relaxivity.

It is noteworthy that Gd(NETA) and Gd(NPTA) having both a macrocyclic and acyclic binding moiety display considerably enhanced T_1 relaxivity as compared to Gd(DTPA) and Gd-(DOTA) and the other new agents evaluated in the present study. For example, the T_1 relaxivities of Gd(NETA), Gd(NPTA), Gd(DTPA), and Gd(DOTA) at 61 MHz are 4.83, 4.66, 4.32, and 3.84, respectively. Like DOTA and DTPA, NETA and NPTA possess eight potential coordinating groups. Unlike DOTA and DTPA, NETA and NPTA possess both macrocyclic and acyclic binding moieties. Since the number of coordinated water molecules ($q = 1$) is the same for all complexes reported,[15] enhanced relaxivities of Gd(NETA) and Gd(NPTA) compared to DOTA and DTPA may be ascribed to the presence of both the macrocyclic and acyclic moieties. All of the flexible acyclic pendant binders may or may not participate in binding Gd(III). Increase in q values of the Gd(III) complexes of bimodal ligands, NETA and NPTA, could occur from a decrease in the ligand denticity from eight- to seven-coordinate by one of the pendent coordinating groups not being coordinated at all or from an "on"−"off" mechanism of one of the pendent coordinating groups. These types of binding to Gd(III) of one of the pendent coordinates would have resulted in enhanced relaxivity of Gd(NETA) and Gd(NPTA), providing values that are intermediate between one coordinated water molecule ($q = 1$) and two coordinated water molecules ($q = 2$).

Gd(DTPA) displayed slightly higher T_1 and T_2 relaxivities at all of the field strengths as compared to the Gd(III) complexes of azepane and piperidine-backbone DTPA. The T_1 and T_2 relaxivities of Gd(DOTA) have been significantly reduced by the addition of a piperidine ring into the system (PIP−DOTA). The addition of a piperidine or azepane ring into DTPA or DOTA resulted in a decrease in both T_1 and T_2 relaxivities. In particular, a high degree of rigidity present in Gd(PIP−DOTA) might lead to significantly reduced relaxivity as compared to that in Gd(DOTA). It is interesting to note that at high field strengths (greater than 10 MHz in units of the proton Larmor frequency), T_1 relaxivities of Gd(PIP−DTPA) are very similar to those of Gd(DOTA).

Serum Stability. The stability of the corresponding [153]Gd-labeled complexes in human serum was assessed by measuring the release of [153]Gd from the complexes at 37 °C over 14 days. The serum stability of [153]Gd-labeled complexes thereby obtained is shown in Figure 5. The chelates PIP−DTPA, PIP−DOTA, and NETA sequestered [153]Gd as the complex in serum with no
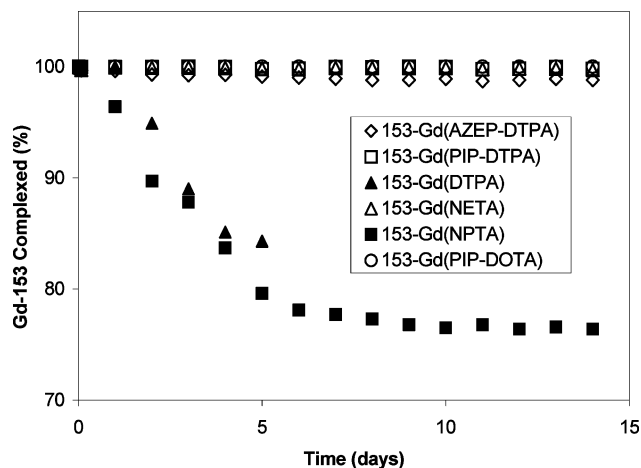

Figure 5. Serum stability of [153]Gd(NETA) (△), [153]Gd(NPTA) (■), [153]-Gd(AZEP−DTPA) (◇), [153]Gd(PIP−DTPA) (□), [153]Gd(DTPA) (▲), and [153]Gd(PIP−DOTA) (○) at pH 7 and 37 °C. The data for [153]Gd(AZEP−DTPA), [153]Gd(PIP−DTPA), and [153]Gd(DTPA) were previous results from ref 9a.

measurable loss of radioactivity over 14 days. A number of reports have shown that Gd(DOTA) is exceptionally stable in human serum.[2] In contrast, there is a rapid loss of [153]Gd from Gd(DTPA) with ~15% released after 5 days. The behavior of the Gd(NPTA) complex mirrors that of Gd(DTPA), i.e., a pronounced loss (>20%) over the first 6 days. The Gd(AZEP−DTPA) also shows evidence of steady metal transfer to serum proteins, although the loss is much more gradual than noted with DTPA or NPTA. The [153]Gd-labeled complexes of the piperidine-backboned chelates are exceptionally stable in serum. Incorporation of the rigid piperidine ring into the DTPA system seems to confer a significant effect on the complex stability in serum. Somewhat surprisingly, the structurally similar chelates NETA and NPTA have markedly different serum stabilities. A considerable release of radioactivity was observed from the [153]Gd(III) complex formed with NPTA which has a propylene chain linking the pendent donor groups to the macrocycle. However, no measurable loss of radioactivity was observed from [153]Gd(NETA) which has an ethylene chain versus the propylene of NPTA. The stability of the Gd(III) radiolabeled complex in serum appears to be dependent on the carbon chain length between the pendent donor groups and the macrocyclic ring in NETA or NPTA. The observed release of radioactivity from NPTA might be a consequence of the formation of a six-membered chelate ring as opposed to what is generally considered to be the more favorable arrangement of donors, i.e., a five-membered chelate ring for complexation of Gd(III).

In Vivo Biodistribution of [153]Gd-Labeled Complexes. A biodistribution study of the chelates was performed in athymic mice to evaluate the in vivo stability of the [153]Gd-labeled chelates. For comparison purposes, a biodistribution of [153]Gd-labeled DOTA was also performed. The results of the biodistribution studies for the new [153]Gd-labeled chelates and [153]Gd-(DOTA) are shown in Table 1. If [153]Gd is released from the chelate, radioactivity would be expected to accumulate in the bone, i.e., the femur, primarily. As a point of interest, the blood and kidney data are included, which are representative of whole body clearance. Radioactivity accumulated in selected organs or cleared from the blood compartment was measured at five time points, 0.5, 1, 4, 8, and 24 h postinjection of the [153]Gd-labeled complexes. The data are presented as the percent injected dose per gram (% ID/g) calculated for blood and selected organs. Examination of the data indicates that [153]Gd(NETA), [153]Gd-

Table 1. Biodistribution of ^{153}Gd-Labeled Chelates in Balb/c Mice Following Intravenous Injection[a]

| | | time points | | | | | | | | | | | | |
| | | 0.5 h | | | 1 h | | | 4 h | | | 8 h | | | 24 h | | |
ligand	tissue															
PIP−DTPA	blood	0.79	±	0.10	0.05	±	0.02	0.01	±	0.01	0.00	±	0.00	0.00	±	0.00
	liver	1.09	±	0.10	0.78	±	0.11	0.50	±	0.08	0.43	±	0.02	0.37	±	0.04
	spleen	0.30	±	0.10	0.09	±	0.01	0.08	±	0.01	0.06	±	0.01	0.05	±	0.00
	kidney	2.96	±	1.28	1.36	±	0.11	1.16	±	0.20	0.88	±	0.06	0.47	±	0.17
	lung	0.57	±	0.23	0.17	±	0.01	0.60	±	0.78	0.11	±	0.03	0.23	±	0.28
	heart	0.43	±	0.08	0.09	±	0.03	0.06	±	0.01	0.05	±	0.02	0.02	±	0.00
	femur	2.31	±	1.39	1.36	±	1.04	0.46	±	0.25	0.29	±	0.15	0.20	±	0.03
PIP−DOTA	blood	0.44	±	0.22	0.13	±	0.03	0.01	±	0.00	0.00	±	0.00	0.00	±	0.00
	liver	0.71	±	0.21	1.16	±	0.63	0.54	±	0.16	0.37	±	0.07	0.42	±	0.09
	spleen	0.18	±	0.09	0.09	±	0.01	0.06	±	0.01	0.04	±	0.01	0.04	±	0.01
	kidney	1.83	±	0.65	1.28	±	0.33	0.80	±	0.17	0.91	±	0.13	0.66	±	0.15
	lung	0.39	±	0.31	0.20	±	0.04	0.12	±	0.07	0.04	±	0.01	0.03	±	0.00
	heart	0.18	±	0.21	0.02	±	0.035	0.07	±	0.04	0.00	±	0.02	0.00	±	0.01
	femur	0.64	±	0.14	0.48	±	0.081	0.30	±	0.11	0.15	±	0.01	0.22	±	0.03
DOTA	blood	0.96	±	0.32	0.37	±	0.27	0.01	±	0.00	0.02	±	0.02	0.00	±	0.00
	liver	1.37	±	0.30	1.03	±	0.35	0.29	±	0.09	0.35	±	0.06	0.15	±	0.02
	spleen	0.40	±	0.12	0.18	±	0.04	0.10	±	0.05	0.17	±	0.07	0.04	±	0.01
	kidney	4.16	±	1.17	2.87	±	0.83	1.55	±	0.50	3.47	±	1.91	1.12	±	0.22
	lung	0.89	±	0.37	0.33	±	0.11	0.09	±	0.06	0.08	±	0.01	0.04	±	0.01
	heart	0.60	±	0.16	0.62	±	0.70	0.07	±	0.08	0.03	±	0.01	0.02	±	0.01
	femur	0.87	±	0.40	0.42	±	0.08	0.11	±	0.05	0.08	±	0.02	0.08	±	0.01
AZEP−DTPA	blood	4.05	±	0.97	2.08	±	0.43	0.20	±	0.02	0.15	±	0.08	0.07	±	0.03
	liver	11.14	±	1.54	13.08	±	1.17	16.99	±	1.65	20.73	±	1.42	19.19	±	1.57
	spleen	2.81	±	0.69	2.37	±	0.39	1.56	±	0.15	1.55	±	0.29	3.25	±	0.91
	kidney	13.41	±	1.09	8.43	±	6.85	10.67	±	6.88	9.66	±	4.92	14.96	±	8.43
	lung	3.80	±	0.68	10.15	±	10.86	4.04	±	1.74	2.18	±	0.34	1.77	±	0.33
	heart	2.97	±	0.55	2.25	±	0.24	3.14	±	2.37	1.19	±	0.08	1.45	±	0.39
	femur	9.00	±	1.39	10.22	±	0.75	15.23	±	5.98	12.87	±	1.94	13.65	±	1.96
NETA	blood	1.31	±	0.15	0.54	±	0.04	0.00	±	0.00	0.00	±	0.00	0.00	±	0.00
	liver	0.56	±	0.05	0.37	±	0.03	0.11	±	0.05	0.08	±	0.01	0.03	±	0.00
	spleen	0.35	±	0.04	0.85	±	0.86	0.29	±	0.35	0.27	±	0.26	0.04	±	0.01
	kidney	3.89	±	0.43	1.88	±	0.41	2.12	±	1.14	0.87	±	0.16	0.59	±	0.07
	lung	0.92	±	0.11	0.46	±	0.12	0.05	±	0.01	0.05	±	0.02	0.03	±	0.01
	heart	0.51	±	0.07	0.25	±	0.07	0.02	±	0.00	0.03	±	0.01	0.02	±	0.00
	femur	1.06	±	0.20	0.56	±	0.33	0.11	±	0.07	0.10	±	0.05	0.03	±	0.00
NPTA	blood	1.60	±	0.37	0.45	±	0.20	0.04	±	0.01	0.04	±	0.02	0.02	±	0.01
	liver	2.78	±	0.39	2.90	±	0.33	3.11	±	0.78	5.09	±	1.35	2.89	±	0.31
	spleen	1.04	±	0.18	2.21	±	2.44	0.69	±	0.18	1.23	±	0.40	0.70	±	0.20
	kidney	14.06	±	3.86	11.63	±	1.80	14.81	±	3.91	12.05	±	3.22	6.80	±	1.45
	lung	1.32	±	0.20	0.72	±	0.22	0.26	±	0.04	0.45	±	0.09	0.32	±	0.03
	heart	0.96	±	0.27	0.47	±	0.11	0.41	±	0.23	0.34	±	0.09	0.20	±	0.05
	femur	3.74	±	0.79	2.80	±	0.43	1.78	±	0.43	2.29	±	0.64	1.84	±	0.22

[a] Values are the percent injected dose per gram (% ID/g) ± standard deviation.

(PIP−DTPA), and ^{153}Gd(PIP−DOTA) display in vivo stability comparable to that of ^{153}Gd(DOTA), while ^{153}Gd(AZEP−DTPA) and ^{153}Gd(NPTA) undergo in vivo dissociation with the former exhibiting the greatest degree of ^{153}Gd transfer. At 4 h postinjection, the liver % ID/g values are 0.50 ± 0.08, 0.54 ± 0.16, 0.29 ± 0.09, and 0.11 ± 0.05 for the ^{153}Gd complexes of PIP−DTPA, PIP−DOTA, DOTA, and NETA, respectively. These Gd(III) complexes display uniformly low bone-uptake which is promising considering that Gd(III) is a bone-seeking metal.[17] In addition, the data indicate a rapid blood clearance for the new Gd(III) complexes. The control species ^{153}Gd-(DOTA) displays higher radioactivity levels in the kidney than in other organs, although the values (<5% ID/g) are still low on an overall scale. Data obtained with ^{153}Gd(NETA) parallel that noted with the DOTA analogue. ^{153}Gd(PIP−DOTA) exhibits lower radioactivity levels in blood and the organs over all time points compared to ^{153}Gd(PIP−DTPA), ^{153}Gd(NETA), and ^{153}Gd(DOTA). It is noteworthy that ^{153}Gd(PIP−DOTA) and ^{153}Gd(PIP−DTPA) display a decreased kidney-to-liver ratio (up to 5.7 times lower) as compared to Gd(DOTA) and Gd(NETA) at all time points. At 0.5 h postinjection, the ratios for ^{153}Gd-(PIP−DOTA), ^{153}Gd(PIP−DTPA), Gd(DOTA), and Gd(NETA) are 2.58, 2.72, 3.04, and 6.95, respectively (Table 2), and kidney retention of piperdine-backboned DOTA and DTPA ^{153}Gd(PIP−

DOTA), ^{153}Gd(PIP−DTPA), and ^{153}Gd(DOTA) was 1.83, 2.96, and 4.16, respectively. However, the difference in kidney retention between these chelates was gradually larger over time and maximized at 24 h, wherein the kidney-to-liver ratios for ^{153}Gd(PIP−DTPA), Gd(PIP−DOTA), and Gd(DOTA) are 1.27, 1.57, and 7.45, respectively (Table 2). Incorporation of the liphophilic piperidine ring into the chelate may account for a modest increase in liver uptake of ^{153}Gd(PIP−DOTA) and ^{153}Gd(PIP−DTPA).

As predicted from the in vitro data, Gd(NPTA) was confirmed to be unstable in vivo as well, and high radioactivity levels in the kidney and liver at 24 h were observed. ^{153}Gd−AZEP−DTPA also clearly undergoes dissociation in vivo resulting in significant radioactivity accumulation in the liver and bone. These chelates have unacceptable stabilities and do not warrant further evaluation. The results of the biodistribution studies as a whole indicate that ^{153}Gd−NETA, ^{153}Gd−PIP−DTPA, and ^{153}Gd−PIP−DOTA display comparable in vivo stability to ^{153}Gd−DOTA and that these chelates might be further exploited for use as MRI contrast agents. In particular, the in vivo biodistribution results of ^{153}Gd−PIP−DTPA and ^{153}Gd−PIP−DOTA indicate that incorporation of the lipophilic piperidine ring provides a measurable effect on liver uptake of these two chelates as evidenced by reduced kidney-to-liver ratio as

Table 2. Biodistribution of [153]Gd-Labeled Chelates in the Liver and the Kidney[a]

| | | time points | | | | |
complexes	tissue	0.5 h	1 h	4 h	8 h	24 h
[153]Gd(DOTA)	liver	1.37 ± 0.30	1.03 ± 0.35	0.29 ± 0.09	0.35 ± 0.06	0.15 ± 0.02
	kidney	4.16 ± 1.17	2.87 ± 0.83	1.55 ± 0.50	3.47 ± 1.91	1.12 ± 0.22
[153]Gd(PIP−DOTA)	liver	0.71 ± 0.21	1.16 ± 0.63	0.54 ± 0.16	0.37 ± 0.07	0.42 ± 0.09
	kidney	1.83 ± 0.65	1.28 ± 0.33	0.80 ± 0.17	0.91 ± 0.13	0.66 ± 0.15
[153]Gd(PIP−DTPA)	liver	1.09 ± 0.10	0.78 ± 0.11	0.50 ± 0.08	0.43 ± 0.02	0.37 ± 0.04
	kidney	2.96 ± 1.28	1.36 ± 0.11	1.16 ± 0.20	0.88 ± 0.16	0.47 ± 0.17
[153]Gd(NETA)	liver	0.56 ± 0.18	0.37 ± 2.44	0.00 ± 0.18	0.08 ± 0.40	0.03 ± 0.20
	kidney	3.89 ± 0.43	1.88 ± 0.41	2.12 ± 1.14	0.87 ± 0.16	0.59 ± 0.07

[a] Values are the percent injected dose per gram (% ID/g) ± standard deviation.

compared to the results of [153]Gd-DOTA. The strategy of backbone modification, in this case adding a lipophilic piperidine ring into the system, appears to provide an entry point for modification of the biological uptake properties of macrocyclic MRI contrast agents.

Conclusion

A series of chelates, PIP−DOTA, PIP−DTPA, AZEP−DTPA, NETA, and NPTA, were prepared and their potential as MRI contrast enhancement agents was assessed. A novel piperidine-backboned DOTA derivative, PIP−DOTA, was synthesized based on a high dilution cyclization method. The serum stability, relaxivity, and in vivo biodistribution of the Gd(III) complexes of the new chelates were investigated and compared to the clinically used MRI contrast agents Gd(DOTA) and Gd(DTPA).

At clinically relevant field strengths, the T_1 and T_2 relaxivities of the new Gd(III) complexes compared favorably to the contrast agents, Gd(DTPA) and Gd(DOTA). It is noteworthy that among the evaluated Gd(III) complexes, Gd(NETA) and Gd(NPTA) having both macrocyclic and acyclic binding moiety displayed the highest T_1 relaxivities at 61 MHz indicating considerably enhanced relaxivity compared to Gd(DTPA) and Gd(DOTA). Serum stability studies show that the novel Gd(III)-labeled complexes, [153]Gd(NETA), [153]Gd(PIP-DTPA), and [153]Gd(PIP-DOTA), were stable in serum for up to 14 days without any measurable loss of radioactivity, a very promising result as the clinically used Gd(DTPA) released 20% of [153]Gd after 5 days. However, [153]Gd(NPTA) was found to be unstable in serum as indicated by a ~15% loss of [153]Gd from NPTA over 5 days. The results obtained from the biodistribution studies indicate that [153]Gd(NETA), [153]Gd(PIP−DTPA), and [153]Gd(PIP−DOTA) possess in vivo stability similar to the analoguous [153]Gd(DOTA), while [153]Gd(AZEP−DTPA) and Gd(NPTA) dissociated in vivo as evidenced by high accumulation of radioactivity in the organs.

The relaxivity and in vitro and in vivo stability data suggest that PIP−DOTA, NETA, and PIP−DTPA may be effective Gd-(III) chelates for use in MRI. The Gd(III) complexes of the piperidine backboned PIP−DOTA and PIP−DTPA display reduced kidney accumulation with respect to the nonspecific Gd(DOTA). The strategy to increase lipophilicity and rigidity of the chelate system and thus enhance hepatobiliary clearance and complex stability by incorporating either a piperidine or an azepane ring into the DTPA system appears promising for the design of liver specific MRI contrast agents. Further evaluations of these two complexes, Gd(PIP−DTPA) and Gd-(PIP−DOTA), along with Gd(NETA) for use as MRI liver agents or nonspecific agents are planned.

Experimental Section

General. ^{1}H, ^{13}C, and APT NMR spectra were obtained using a Varian Gemini 300 instrument, and chemical shifts are reported in ppm on the δ scale relative to tetramethylsilane (TMS). Proton

chemical shifts are annotated as follows: ppm (multiplicity, integral, coupling constant (Hz)). Fast atom bombardment mass spectra (FAB-MS) were obtained on an Extrel 4000 in the positive ion detection mode. Melting points were obtained on Mel-Temp (Laboratory Device Inc., Dubuque, IA). Chromatograms (SE-HPLC) were obtained on a Lab Alliance Qgrad isocratic system with a Waters 717 plus autosampler, a Gilson 112 UV detector, and an in-line IN/US γ-Ram model 2 radiodetector. Elemental microanalyses were performed by Galbraith Laboratories, Knoxville, TN. HRMS analyses of compound **7** was performed by the Laboratory of Analytical Chemistry (Dr. Sonja Hess, NIDDK, Bethesda, MD). HRMS analyses of compound **8** and **9** were performed by the mass spectrometry laboratory at the University of Notre Dame, IN. PIP−DTPA,[9a] AZEP−DTPA,[9a] NETA,[9b] and NPTA[9b] were synthesized as described previously. Gd(DTPA) was used as its *N*-methylglucamine salt, also known as gadopentate dimeglumine (Magnevist), and was obtained from Berlex Laboratories, Wayne, NJ. Gd(DOTA) (Dotarem) was obtained from Guerbet LLC (Bloomington, IN). The [153]Gd was obtained from Isotope Products, Valencia, CA. Phosphate buffered saline (PBS), 1X, pH 7.4 consisted of 0.08 M Na_2HPO_4, 0.02 M KH_2PO_4, 0.01 M KCl, and 0.14 M NaCl. Caution: [153]Gd ($t_{1/2}$ = 241.6 days) is a γ-emitting radionuclide. Appropriate shielding and handling protocols should be in place when using this isotope.

N-Carbobenzoxy-piperidine-*cis*-2,6-dicarboxylic Acid 2. To a solution of 2,6-pyridinedicarboxylic acid (25 g, 0.15 mmol) in 2 M NaOH (160 mL) and water (40 mL) was added 5% Rh/alumina catalyst (2.5 g). The resulting mixture was subjected to hydrogenation by agitation with excess $H_2(g)$ at 45 psi in a Parr hydrogenation apparatus at ambient temperature for 24 h. The reaction mixture was filtered through Celite, and the Celite was washed with water (100 mL). The filtrate was cooled to 0 °C, and 2 M NaOH (63 mL) and CBZ−Cl (35.2 mL, 0.21 mmol) were added into the filtrate. The resulting mixture was allowed to warm to room temperature and stirred for 18 h. The aqueous layer was washed with ethyl ether (200 mL), adjusted to pH 2.5−3 with 3 M HCl, and extracted with EtOAc (2 × 300 mL). The combined EtOAc layers were washed with water (2 × 200 mL) and saturated NaCl solution (200 mL), dried (MgSO$_4$), filtered, and evaporated. The residue was dissolved into EtOAc (50 mL), and hexanes (300 mL) were added to the solution. The resulting slurry was placed in the freezer for 4 h. The white precipitate was filtered and dried under vacuum to provide pure **2** as a white solid (36.9 g, 76%). The ^{1}H and ^{13}C NMR spectra of the material thereby obtained are essentially identical to data reported previously for **2**:[13] mp = 172 °C;^{1}H NMR (DMSO) δ 1.51−1.69 (m, 4 H), 2.01 (d, *J* = 7.1 Hz, 2 H), 4.65 (d, *J* = 4.3 Hz, 2 H), 5.11 (s, 2 H), 7.30−7.36 (m, 5 H); ^{13}C NMR (DMSO) δ 16.3 (t), 25.5 (t), 52.9 (d), 66.9 (t), 127.3 (d), 128.0 (d), 128.4 (d), 136.6 (s), 155.5 (s), 173.4 (s).

N-Carbobenzoxy-*cis*-2,6-bis(succinimidylcarbonyl)piperidine 3. A mixture of **2** (27.6 g, 85 mmol), *N*-hydroxysuccinimide (20.7 mmol, 180 mmol), EDC (34.5 g, 180 mmol) in EtOAc (375 mL), and DMF (375 mL) was stirred for 18 h. The active ester **3** precipitated during the reaction was filtered. The filtrate was washed with water (300 mL), 1 M NaHCO$_3$ (2 × 300 mL), and 1 M HCl (2 × 300 mL). Additional EtOAc (150 mL) was added to dissolve the white precipitate formed during extractions. The combined EtOAc layer was dried (MgSO$_4$), filtered, and evaporated in vacuo.

The residue was crystallized from EtOAc/hexanes and placed in the freezer. The white precipitate was filtered. The combined precipitate was dried on high vacuum to provide pure **3** (35.2 g, 78%): mp = 196 °C; ^{1}H NMR (DMSO) δ 1.63–1.74 (m, 2 H), 2.09 (d, J = 8.3 Hz, 4 H), 3.36 (s, 1 H), 5.02 (t, J = 7.2 Hz, 2 H), 5.15 (s, 2 H), 7.31–7.42 (m, 5 H); ^{13}C NMR (DMSO) δ 15.8 (t), 25.5 (t), 51.8 (d), 67.4 (t), 127.6 (d), 127.9 (d), 128.4 (d), 136.0 (s), 155.2 (d), 167.2 (s), 170.0 (s). Anal. Calcd for $C_{23}H_{23}N_3O_{10}$: C, 55.09; H, 4.62. Found: C, 54.76; H, 4.78.

(1S,11R)-2,5,10-Trioxo-3,6,9,15-tetraaza-bicyclo[9.3.1]-pentadecane-15-carboxylic Acid Benzyl Ester 5. To dioxane (1.5 L) at 90 °C was added a solution of active succinimide ester **3** (2.5 g, 5 mmol) in DMSO (30 mL) and a solution of diamine **4** (585 mg, 5 mmol) in DMF (30 mL), each taken up into 100 mL in a gastight syringe over 24 h. Four more additions of each 5 mmol solutions were added over 4 days. After the fifth addition, the reaction was heated for 24 h, cooled to room temperature, and concentrated in vacuo. The thick brown residue was dissolved in CH_2Cl_2 (300 mL). The CH_2Cl_2 layer was washed with H_2O (2 × 100 mL), 1 M HCl (2 × 100 mL), brine (2 × 100 mL), 1 M NaHCO$_3$ (2 × 100 mL), and water (2 × 100 mL). The combined CH_2Cl_2 layers were dried (MgSO$_4$), filtered, and evaporated to dryness. The residue was purified via column chromatography on silica gel by eluting with 3% CH$_3$OH–CH$_2$Cl$_2$. Pure **5** (1.03 g, 53%) was thereby obtained as a white solid: mp = 182 °C; ^{1}H NMR (CDCl$_3$) δ 1.48–1.62 (m, 3 H), 1.95–2.4 (m, 4 H), 3.03–3.27 (m, 3H), 3.44–3.82 (m, 2 H), 4.23–4.42 (m, 1 H), 4.69–4.86 (m, 2 H), 5.11 (d, J = 9.8 Hz, 1 H), 5.42 (d, J = 9.8 Hz, 1 H), 5.63 (s, 0.6 H), 6.29 (s, 0.4 H), 6.56 (s, 0.4 H), 6.71 (s, 0.6 H), 7.30–7.56 (m, 5 H); ^{13}C NMR (CDCl$_3$) δ 16.0 (t), 17.9 (t), 23.9 (t), 24.0 (t), 24.2 (t), 36.9 (t), 37.1 (t), 37.6 (t), 37.7 (t), 44.2 (t), 51.2 (d), 51.7 (d), 52.4 (d), 53.0 (d), 57.4 (t), 68.2 (t), 68.5 (t), 127.8 (d), 127.9 (d), 128,2 (d), 128.4 (d), 135.2 (s), 156.2 (s), 156.4 (s), 170.2 (s), 170.9 (s), 171.3 (s), 171.4 (s), 171.5 (s), 171.9 (s). Anal. Calcd for $C_{19}H_{24}N_4O_5$: C, 58.75; H, 6.23. Found: C, 59.06; H, 6.51.

(1S,11R)-3,6,9,15-Tetraaza-bicyclo[9.3.1]pentadecane-2,5,10-trione 6. To a solution of **5** (1.0 g, 2.57 mmol) in EtOH (30 mL) was added 10% Pd/C catalyst (200 mg). The resulting mixture was subjected to hydrogenation by agitation with excess H_2(g) at 30 psi in a Parr hydrogenation apparatus at ambient temperature for 3 h. The reaction mixture was filtered through Celite, and the filtrate was concentrated in vacuo. The residue was purified via column chromatography on neutral alumina and was eluted with 10% CH$_3$OH–EtOAc. Pure **6** (630 mg, 97%) was thereby obtained as a white solid: ^{1}H NMR (CDCl$_3$) δ 1.61–1.74 (m, 4 H), 2.00–2.06 (m, 2 H), 3.21–3.41 (m, 3 H), 3.54–3.74 (m, 4 H), 3.90 (d, J = 14.1 Hz, 1 H); ^{13}C NMR (CDCl$_3$) δ 19.4 (t), 26.5 (t), 27.2 (t), 40.1 (t), 40.4 (t), 47.1 (t), 54.9 (d), 55.6 (d), 176.7 (s), 179.3 (s), 179.6 (s). Anal. Calcd for $C_{11}H_{18}N_4O_3(H_2O)_{0.5}$: C, 51.05; H, 7.21. Found: C, 50.89; H, 7.21.

(1R,11S)-3,6,9,15-Tetraaza-bicyclo[9.3.1]pentadecane 7. To a slurry of **6** (540 mg, 2.12 mmol) in THF (20 mL) at 0 °C under argon was added dropwise 2 M BH$_3$–Me$_2$S (9.6 mL, 9.6 mmol) over 1 h. The resulting mixture was stirred at 0 °C for 1 h and at room temperature for 2 h and was refluxed for 5 days. The reaction was cautiously quenched by dropwise addition of 10% H_2O/THF (1 mL), and the reaction mixture was concentrated. The residue was treated with CH$_3$OH (30 mL) and evaporated. This was repeated twice, and the residue was applied to high vacuum for 2 h and was treated with 6 M HCl (5 mL). The resulting mixture was refluxed for 1 h, cooled to room temperature, and washed with CHCl$_3$ (2 × 50 mL). The pH of the aqueous solution was adjusted to 13 with 5 M NaOH, and the solution was extracted with CHCl$_3$ (3 × 100 mL). The combined CHCl$_3$ layers were dried, filtered, and evaporated to provide pure **7** (248 mg, 55%) as a colorless oil: ^{1}H NMR (D$_2$O) δ 1.12–1.82 (m, 8 H), 2.96–3.42 (m, 16 H); ^{13}C NMR (D$_2$O) δ 22.3 (t), 26.6 (t), 44.4 (t), 45.2 (d), 49.7 (t), 52.0 (t). HRMS (positive ion FAB): calcd for $C_{11}H_{24}N_4$, [M + H]$^+$ m/z 213.2097; found, [M + H]$^+$ m/z 213.2083.

{(1R,11S)-6,9,15-Tris-*tert*-butoxycarbonylmethyl-3,6,9,15-tetraaza-bicyclo[9.3.1]pentadec-3-yl}-acetic Acid *tert*-Butyl Ester 8. To a slurry of **7·HCl** (92 mg, 0.26 mmol) in DMF (3 mL) at 0 °C was added DIPEA (445 mg, 3.44 mmol), KI (68 mg, 0.41 mmol), and *tert*-butyl bromoacetate (220 mg, 11.3 mmol). The resulting mixture was stirred for 2 h at 0 °C and for 2 h at room temperature. The reaction mixture was heated to 90 °C and stirred for 18 h, cooled to room temperature, and concentrated in vacuo. The solvent was evaporated, and the residue was purified via column chromatography on silica gel eluting with 15% CH$_3$OH–CH$_2$Cl$_2$. Pure **8** (65 mg, 37%) was thereby obtained as a colorless oil: ^{1}H NMR (CDCl$_3$) δ 1.32–1.56 (m, 36 H), 1.75–1.98 (m, 4 H), 2.30–2.42 (m, 2 H), 2.60–3.04 (m, 8 H), 3.21–3.60 (m, 10 H), 4.02–4.09 (m, 2 H); ^{13}C NMR (CDCl$_3$) δ 20.2 (t), 26.0 (t), 28.1 (q), 51.4 (t), 52.2 (t), 52.7 (t), 53.2 (t), 54.3 (t), 56.0 (t), 56.2 (t), 57.7 (t), 80.5 (s), 80.6 (t), 80.7 (t), 170.5 (s), 170.7 (s), 171.1 (s). HRMS (positive ion FAB): calcd for $C_{35}H_{64}N_4O_8Na$, [M + Na]$^+$ m/z 691.4635; found, [M + Na]$^+$ m/z 691.4622.

[(1R,11S)-6,9,15-Tris-carboxymethyl-3,6,9,15-tetraaza-bicyclo-[9.3.1]pentadec-3-yl]-acetic Acid 9. A solution of **8** (110 mg, 0.17 mmol) in ice–water bath was treated with 4 M HCl in 1,4-dioxane (5 mL). The mixture was allowed to warm to ambient temperature and then was stirred for 18 h. The precipitate was collected and washed with ethyl ether. The collected solid was dissolved in water immediately and lyophilized to provide pure **9** (PIP–DOTA) as a white solid (66 mg, 87%): ^{1}H NMR (D$_2$O) δ 1.43–1.54 (m, 2 H), 1.62–2.07 (m, 4 H), 3.16 (s, 6 H), 3.24–3.56 (m, 4 H), 3.74 (s, 2 H), 3.90 (s, 4 H), 4.06 (s, 2 H); ^{13}C NMR (D$_2$O) δ 18.78 (t), 32.14 (t), 53.0 (t), 53.4 (t), 53.5 (t), 54.2 (t), 56.8 (t, 2C), 57.0 (t), 57.7 (t), 57.9 (t), 170.0 (s), 172.5 (s), 175.0 (s). HRMS (positive ion FAB): calcd for $C_{19}H_{31}N_4O_8$, m/z 443.2153; found, m/z 443.2142.

Measurements of Relaxivity. NMR dispersion measurements were made on a custom-designed variable field T_1–T_2 analyzer (Southwest Research Institute, San Antonio, TX) at 23 °C. The magnetic field was varied from 0.02 to 1.5 T (corresponding to a proton Larmor frequency of 1–64 MHz). T_1 was measured by using a saturation recovery pulse sequence with 32 incremental recovery times. The relaxivities (relaxation rates per mM Gd(III) concentration) were obtained after subtracting the water contribution. The commercial Gd(DTPA) (Magnevist) and Gd(DOTA) (Dotarem) were used without further modifications. The other Gd chelates were prepared by dissolving the appropriate ligand and GdCl$_3$ at a 1:0.9 mole ratio in water with stirring and by adjusting the pH of the resulting solution to 6.5 with 1 M NaOH. The total Gd concentration for each sample was determined by ICP-AAS (Desert Analytics, Tuscon, AZ).

Serum Stability. The ^{153}Gd-labeled complexes of the new chelates, PIP–DOTA, NETA, and NPTA, were prepared by the addition of 200 μL/350 μCi of ^{153}Gd (0.1 M HCl with the pH adjusted to 4.5 with 5 M NH$_4$OAc) to a small tube containing 200 μL of a 7 μmol ligand solution in 0.15 M NH$_4$OAc of pH 4.5. The reaction tube was capped, and the mixture was heated at 80 °C for 12 h. The mixture was loaded onto a column of Chelex-100 resin (1 mL volume bed, equilibrated with phosphate-buffered saline (PBS), pH 7.4). The complexes were eluted from the resin with PBS, pH 7.4, while the resin retained free ^{153}Gd. Radiolabeled complexes were diluted to an appropriate volume that allowed for preparation of multiple samples containing 5–10 μCi and were filter-sterilized using a Millex-GV 0.22 μm filter. This stock solution was then mixed with 1400 μL of human serum. Aliquots (200 μL) were drawn and separated into individual tubes for subsequent analysis using aseptic technique. All samples awaiting analysis were stored at 37 °C in a CO$_2$ incubator. An aliquot of the mixture (30–50 μL) was taken at selected times (Figure 4) and analyzed by SE-HPLC. The serum stability of the ^{153}Gd complexes was assessed by measuring the transfer of the ^{153}Gd from the complexes to serum proteins by use of a SE-HPLC fitted with a TSK 3000 column. Samples were eluted with PBS at a flow rate of 1 mL/min.

In Vivo Biodistribution Studies. Female athymic mice were obtained from Charles River Laboratories (Wilmington, MA) at 4–6 weeks of age. The pH of the ^{153}Gd-labeled ligands was adjusted

to pH ~7.0 with 0.5 M sodium bicarbonate (pH 10.5) and diluted in phosphate-buffered saline. The radiolabeled ligands (5−7 μCi) were administered to the mice in 200 μL of solution via tail vein injection. The mice (five per data point) were sacrificed by exsanguination at 0.5, 1, 4, 8, and 24 h. Blood and the major organs were harvested and wet-weighed, and the radioactivity was measured in a γ-scintillation counter (Minaxi-γ; Packard, Downers Grove, IL). The percent injected dose per gram (% ID/g) was determined for each tissue. The values presented are the mean and standard deviation for each tissue. All animal experiments were performed in compliance with current regulations and guidelines of the U.S. Department of Agriculture and approved by the NCI Animal Care and Use Committee.

References

(1) (a) Padhani, A. R. Dynamic contrast-enhanced MRI in clinical oncology: current status and future directions. *Magn. Reson. Imaging* **2002**, *16*, 407−422. (b) Wiener, E. C.; Brechbiel, M. W.; Brothers, H.; Magin, R. L.; Gansow, O. A.; Tomalia, D. A.; Lauterbur, P. C. Dendrimer-based metal chelates: a new class of magnetic resonance imaging contrast agents. *Magn. Reson. Med.* **1994**, *31*, 1−8. (c) Moats, R. A.; Fraser, S. E.; Meade, T. J. A smart magnetic resonance imaging agent that reports on specific enzymic activity. *Angew. Chem., Int. Ed. Engl.* **1997**, *36*, 726−728. (d) Sipkins, D. A.; Cheresh, D. A.; Kazemi, M. R.; Nevin, L. M.; Bednarski, M. D.; Li, K. C. Detection of tumor angiogenesis in vivo by $\alpha_{\nu\beta3}$-targeted magnetic resonance imaging. *Nat. Med.* **1998**, *4*, 623−626.

(2) Caravan, P.; Ellison, J. J.; McMurry, T. J.; Lauffer, R. B. Gadolinium-(III) chelates as MRI contrast agents: structure, dynamics, and applications. *Chem. Rev.* **1999**, *99*, 2293−2352.

(3) Aime, S.; Botta, M.; Fasano, M.; Terreno, E. Lanthanide(III) chelates for NMR biomedical applications. *Chem. Soc. Rev.* **1998**, *27*, 19−29.

(4) Banci, L.; Bertini, I.; Luchinat, C. *Nuclear and Electronic Relaxation*; VCH Publishers: Weinheim, Germany,1991.

(5) Yoneda, S.; Emi, N.; Fujita, Y.; Ohmichi, M.; Hirano, S.; Suzuki, K. T. Effects of gadolinium chloride on the rat lung following intratracheal instillation. *Fundam. Appl. Toxicol.* **1995**, *28*, 65−70.

(6) Vogl, T. J.; Lencioni, R.; Hammerstingl, R. M.; Bartolozzi, C. Contrast Agents. *Magnetic Resonance Imaging in Liver Disease*; Georg Thieme Verlag Publisher: Stuttgart, Germany, 2003; Chapter 4.

(7) Reimer, P.; Schneider, G.; Schima, W. Hepatobiliary contrast agents for contrast-enhanced MRI of the liver: properties, clinical development and applications. *Eur. Radiol.* **2004**, *14*, 559−578.

(8) Vogl, T. J.; Hammerstingl, R.; Schwarz, W. Superparamagnetic iron oxide enhanced versus gadolinium-enhanced MR imaging for differential diagnosis of focal liver lesions. *Radiology* **1996**, *198*, 881−887.

(9) (a) Chong, H. S.; Garmestani, K.; Bryant, L. H.; Brechbiel, M. W. Synthesis of DTPA analogues derived from piperidine and azepane: potential contrast enhancement agents for magnetic resonance imaging. *J. Org. Chem.* **2001**, *66*, 7745−7750. (b) Chong, H. S.; Garmestani, K.; Ma, D.; Milenic, D. E.; Overstreet, T.; Brechbiel, M. W. Synthesis and biological evaluation of novel macrocyclic ligands with pendent donor groups as potential yttrium chelators for radioimmunotherapy with improved complex formation kinetics. *J. Med. Chem.* **2002**, *45*, 3458−3464.

(10) (a) Fossheim, R.; Dugstad, H.; Dahl, S. G. Structure−stability relationships of Gd(III) ion complexes for magnetic resonance imaging. *J. Med. Chem.* **1991**, *34*, 819−826. (b) Brechbiel, M. W.; Gansow, O. A. Backbone-substituted DTPA ligands for ^{90}Y radio-imunotherapy. *Bioconjugate Chem.* **1991**, *2*, 187−194.

(11) Schuhmann-Giampieri, G.; Schmitt-Willich, H.; Frenzel, T. Biliary excretion and pharmacokinetics of a gadolinium chelate used as a liver-specific contrast agent for magnetic resonance imaging in the rat. *J. Pharm. Sci.* **1993**, *82*, 799−803.

(12) Denny, W. A.; Atwell, G. J.; Baguley, B. C.; Wakelin, L. P. Potential antitumor agents. 44. Synthesis and antitumor activity of new classes of diacridines: importance of linker chain rigidity for DNA binding kinetics and biological activity. *J. Med. Chem.* **1985**, *28*, 1568−1574.

(13) Guo, C.; Reich, S.; Showalter, R.; Villafranca, E., Dong, L. A concise synthesis of AG5473/5507 utilizing *N*-acyliminium ion chemistry. *Tetrahedron Lett.* **2000**, *41*, 5307−5311.

(14) Chappell, L. L.; Deal, K. A.; Dadachova, E.; Brechbiel, M. W. Synthesis, conjugation, and radiolabeling of a novel bifunctional chelating agent for ^{225}Ac radioimmunotherapy applications. *Bioconjugate Chem.* **2000**, *11*, 510−519.

(15) Kim, W. D.; Kiefer, G. E.; Maton, F.; McMillan, K.; Muller, R. N.; Sherry, A. D. Relaxometry, luminescence measurements, electrophoresis, and animal biodistribution of lanthanide(III) complexes of some polyaza macrocyclic acetates containing pyridine. *Inorg. Chem.* **1995**, *34*, 2233−2243.

(16) Reichert, D. E.; Hancock, R. D.; Welch, M. J. Molecular mechanics investigation of gadolinium(III) complexes. *Inorg. Chem.* **1996**, *35*, 7013−7020.

(17) (a) Beliles, R. P. *Toxicity of Heavy Metals in the Environment;* Oehme, F. W., ed.; Hazardous and Toxic Substances, Parts 1 and 2; Marcel Dekker: New York, 1979; Vol. 2, pp 547−615. (b) Gibby, W. A.; Gibby, K. A. Comparison of Gd DTPA−BMA (Omniscan) versus Gd HP−DO3A (ProHance) retention in human bone tissue by inductively coupled plasma atomic emission spectroscopy. *Invest. Radiol.* **2004**, *39*, 138−142.